Status and future perspective of a-Si:H, a-SiGe:H, and nc-Si:H thin film photovoltaic technology

Jeffrey Yang and Subhendu Guha
United Solar Ovonic LLC, 1100 West Maple Road, Troy, Michigan 48084, USA

ABSTRACT

United Solar Ovonic is world's largest manufacturer of thin film solar laminates that convert sunlight to electricity. In 1997, we attained initial 14.6% and stable 13.0% cell efficiencies using an a-Si:H/a-SiGe:H/a-SiGe:H triple-junction structure, which established the foundation of large volume roll-to-roll production. Since then, the power rating of our standard product has been steadily improving from 128 W to 136 W and 144 W. For future generation high efficiency products, we have investigated the possibility of using nc-Si:H to replace the narrow bandgap a-SiGe:H intrinsic layer in the middle and bottom cells of the triple-junction structure. We have investigated various deposition techniques for improving the nc-Si:H material property, solar cell efficiency, and deposition rate. The triple-junction solar cell efficiency incorporating nc-Si:H in the middle and bottom cells has exceeded the record efficiency previously achieved using the conventional a-Si:H/a-SiGe:H/a-SiGe:H triple-junction structure. However, in order to insert the nc-Si:H technology into large volume production, several important issues need to be addressed and resolved. We are currently focusing on these key technical challenges, including high efficiency, high rate nc-Si:H deposition, and large-area nc-Si:H uniformity. In this paper, we review recent advances in a-Si:H and nc-Si:H based multi-junction solar cells and modules.

Keywords: a-Si:H, nc-Si:H, thin film solar cells, VHF.

1. INTRODUCTION

Hydrogenated amorphous silicon (a-Si:H), silicon germanium (a-SiGe:H), and nanocrystalline silicon (nc-Si:H) are the three major intrinsic layers used in multi-junction silicon-based solar cells [1]. Photovoltaic products made using these materials have captured a significant market share. Different cell structures are used, including a-Si:H single-junction [2], a-Si:H/a-Si:H double-junction [3], a-Si:H/a-SiGe:H double-junction [4], a-Si:H/nc-Si:H double-junction [5-6], a-Si:H/a-SiGe:H/a-SiGe:H triple-junction [7], and a-Si:H/nc-Si:H/nc-Si:H triple-junction structures [8]. Each cell structure has its unique advantage in terms of manufacturing cost and product application. For example, the manufacturing cost of a-Si:H single-junction solar cells is lower than multi-junction solar cells, but it has lower conversion efficiency and poorer light-induced stability known as the Staebler-Wronski effect [9]. On the other hand, multi-junction solar cells perform better than single-junction cells, but its manufacturing process is more complex, thus the manufacturing cost is higher. In the last two decades, several a-Si:H single-junction solar cell manufacturing plants were built. Due to the poorer cell performance, a-Si:H single-junction products could not expand its market share. During the same period, Energy Conversion Devices, Inc. and its subsidiary,United Solar Ovonic (United Solar), developed and launched products based on a spectrum splitting, a-Si:H/a-SiGe:H/a-SiGe:H triple-junction structure. It was demonstrated that the triple-junction solar cell structure resulted in high efficiencies and the product showed reduced light induced degradation after prolonged light soaking. World-record initial and stable cell efficiencies of 14.6% and 13.0% were achieved in 1997 [10]. In the meantime, manufacturing technology by employing a roll-to-roll deposition technique on flexible stainless steel substrates has been continuously improving and capacity expanded from 5MW/year [11] to 30 MW/year in 2003 [7, 12]. Today, United Solar has an annual production capacity of 180 MW.

In recent years, nc-Si:H (also referred to as μc-Si:H in the literature) as an intrinsic absorber layer has attracted a great deal of attention. Spurred by the work of the group at Neuchatel University on nc-Si:H solar cells [13-15], significant progress has been made by many groups around the world [5, 6, 8, 13-19]. To date, both the cell and module efficiencies for multi-junction structures incorporating a-Si:H and nc-Si:H have exceeded the records achieved by using the a-Si:H and a-SiGe:H triple-junction structure. There are two major advantages for using nc-Si:H solar cells: high

Thin Film Solar Technology, edited by Alan E. Delahoy, Louay A. Eldada, Proc. of SPIE Vol. 7409,
74090C · © 2009 SPIE · CCC code: 0277-786X/09/$18 · doi: 10.1117/12.827419

Downloaded from SPIE Digital Library on 04 Jan 2010 to 159.226.100.225. Terms of Use: http://spiedl.org/terms

long wavelength response and low light-induced degradation. However, because of the nature of indirect transition in the crystalline phase, nc-Si:H intrinsic layers are usually made much thicker than the a-Si:H and a-SiGe:H intrinsic layers. For example, the total thickness of typical a-Si:H/a-SiGe:H/a-SiGe:H triple-junction solar cells is about half a micrometer, while the intrinsic layer in a single-junction nc-Si:H solar cell is at least one micrometer. Therefore, high rate deposition is a necessary requirement for manufacturing a-Si:H and nc-Si:H multi-junction solar cells. Although several high rate deposition methods have been proposed, including very high frequency (VHF) [13-18], microwave glow discharge [19-21], thermal expansion plasma [22], and hot-wire chemical vapor deposition [23], VHF is the most promising technique for high rate nc-Si:H deposition. Because of the very high frequency (40-130 MHz), the uniformity of large-area nc-Si:H deposition is a major challenge.

United Solar has been investigating a-Si:H and nc-Si:H multi-junction solar cells since 2001 [24]. Significant progress has been made in material characterization and optimization, solar cell design, and device fabrication. In this paper, the status of a-Si:H and nc-Si:H multi-junction solar cells, issues and challenges, and future perspective will be discussed.

2. AMORPHOUS SILICON AND SILICON GEMANIUM ALLOY TRIPLE-JUNCTION SOLAR CELLS

The key technique of making a-Si:H useful in electronic devices is the hydrogenation, where hydrogen atoms terminate silicon dangling bonds and reduce the defect density from $>10^{18}$ cm^{-3} to $\sim10^{16}$ cm^{-3}. Plasma enhanced chemical vapor deposition (PECVD) or glow discharge is the main technique of decomposing SiH_4, GeH_4, and other doping gases. Deposition parameters, such as substrates temperature, power density, and chamber pressure affect the material quality. However, a key parameter is hydrogen dilution during deposition, which improves the quality of a-Si:H and a-SiGe:H, determines the amorphous/nanocrystalline transition, and controls the crystallinity in nc-Si:H materials. The effect of hydrogen dilution is discussed next.

2.1. Amorphous silicon and silicon germanium properties and material optimization

Optimizations of a-Si:H and a-SiGe:H material quality by tuning the deposition parameters are very complicated because the material quality depends on many deposition parameters and they influence each other. In addition, the optimized parameters could be very different from system to system. However, general guidelines for optimization are still applicable. For example, the substrate temperature should be high enough to allow for high surface mobility of impinging species to find low energy sites to form a solid film. On the other hand, it should be low enough to prevent hydrogen effusion from the deposited film. Compromising the two opposing effects, optimized substrate temperature is typically in the range of 200°C to 300°C. High deposition rates usually require high substrate temperatures. Deposition of heavier species also needs high temperatures. For example, one uses higher substrate temperature for a-SiGe:H than for a-Si:H depositions. The chamber pressure needs to be optimized based on the consideration of ion bombardment to the growth surface and the formation of large particles in the plasma. High pressure reduces ion bombardment but promotes the particle formation. The optimized pressure is normally in the range of one to several torrs for a-Si:H and a-SiGe:H depositions using conventional PECVD. The excitation power should be high enough to sustain stable plasma while maintaining a desired deposition rate, but should be low enough to avoid high ion bombardment. High excitation power usually results in high deposition rate, but causes poor material quality.

Another critical parameter for attaining high quality a-Si:H and a-SiGe:H is hydrogen dilution, which is usually defined as the ratio of the hydrogen flow rate to the active gases, such as SiH_4, Si_2H_6, and GeH_4. Guha *et al.* first reported that hydrogen dilution could reduce the light-induced degradation and improve a-Si:H quality [25]. Since then, hydrogen dilution is widely used for improving the a-Si:H and a-SiGe:H solar cell performance. Figure 1 shows the open-circuit voltage (V_{oc}) as a function of hydrogen dilution ratio (R), where R is a relative number to the optimized a-Si:H solar cell deposition (R=1) [12,26,27]. The three curves represent the series with three different cell thicknesses. One can see that with the increase of hydrogen dilution, the V_{oc} increases slightly, reaching a maximum value before a sharp drop. The dramatic decrease of V_{oc} with the hydrogen dilution is caused by the formation of nanocrystalline path along the film thickness. Due to the strong dependence of the material structure on the plasma condition, when deposition is in the amorphous/nanocrystalline transition regime, the V_{oc} spreads. The material deposited under these conditions is also referred to as mixed-phase material. With further increase of the hydrogen dilution, the V_{oc} reaches ~ 0.5V, a typical

Downloaded from SPIE Digital Library on 04 Jan 2010 to 159.226.100.225. Terms of Use: http://spiedl.org/terms

value for nc-Si:H solar cells. The hydrogen dilution induced amorphous/nanocrystalline transition is a very interesting phenomenon and has received significant attention from both fundamental physics and technology application points of view.

Next we discuss materials made with hydrogen dilution near but before reaching the amorphous/nanocrystalline transition. The material made under such conditions is called the "edge" material or "proto-crystalline" material. The properties of the edge material includes a shift of amorphous Raman peak to higher wave numbers [28], a sharp crystalline Raman peak at certain locations when measured with micro-Raman spectroscopy [29], a red shift from 640 cm^{-1} to 620 cm^{-1} in the IR spectra, and an appearance of linear-like nanostructures or intermediate-ordered structures [28]. The most important characteristics of the edge material in solar cells are the high V_{oc} and improved stability. Table 1 compares a-Si:H and a-SiGe:H solar cell performance, where the cells were deposited on stainless steel substrates with different hydrogen dilution ratios. The results clearly show that the solar cells made with high hydrogen dilution not only have higher initial efficiencies but also are more stable than those deposited with low hydrogen dilution. Hydrogen dilution is routinely used for a-Si:H and a-SiGe:H solar cell deposition in our laboratory and production lines. The general guideline for determining the optimized hydrogen ratio is to first find the amorphous/nanocrystalline transition, and then to reduce the dilution slightly to arrive at the optimum condition for solar cells.

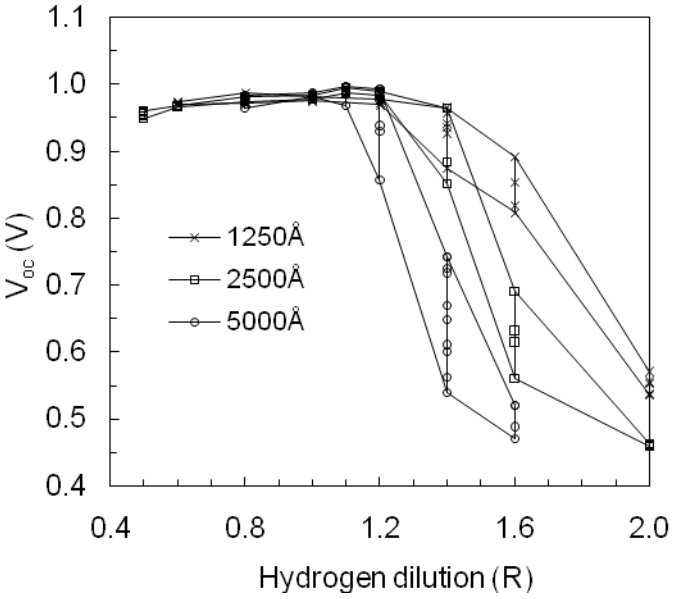

Figure 1. Dependence of V_{oc} on hydrogen dilution for a-Si:H cells with different intrinsic layer thicknesses.

Table 1. Light J-V characteristic of a-Si:H and a-SiGe:H solar cells made with high and low hydrogen dilution ratios, where J_{sc}, V_{oc}, FF, and P_{max} denote short-circuit current density, open-circuit voltage, fill factor, and maximum power.

Description	State	J_{sc} (mA/cm^2)	V_{oc} (V)	FF	P_{max} (mW/cm^2)
a-Si:H, 300°C, low dilution	Initial Degraded	12.3 11.6	0.94 0.91	0.65 0.55	7.5 5.8
a-Si:H, 300°C, high dilution	Initial Degraded	11.6 11.2	0.96 0.94	0.68 0.61	7.6 6.4
a-Si:H, 175°C, low dilution	Initial Degraded	11.4 9.5	0.96 0.91	0.64 0.46	7.0 4.0
a-Si:H, 175°C, high dilution	Initial Degraded	10.9 10.5	1.00 0.97	0.69 0.60	7.5 6.1
a-SiGe:H, low dilution	Initial Degraded	17.6 14.9	0.72 0.64	0.55 0.41	7.1 3.9
a-SiGe:H, high dilution	Initial Degraded	18.0 16.3	0.74 0.69	0.59 0.45	8.0 5.1

Downloaded from SPIE Digital Library on 04 Jan 2010 to 159.226.100.225. Terms of Use: http://spiedl.org/terms

2.2. Single-junction solar cell structures

At United Solar, we use thin flexible stainless steel substrate for terrestrial products and light-weight polymer for space and stratosphere applications. Because the hole mobility is much smaller than the electron mobility in a-Si:H and a-SiGe:H, the *p/i* junction is the dominant junction in a *p-i-n* solar cell structure. Therefore, to obtain high efficiency, the light should enter the solar cell through the p layer instead of the n layer. Based on this consideration, *p-i-n* structures are normally used for solar cells made on transparent-conductive-oxide (TCO) coated superstrates, while *n-i-p* structures are used on non-transparent substrates. For a-Si:H single-junction solar cells, the structure is reasonably simple: the *n, i*, and *p* layers are deposited on the substrates in sequence with special attention paid to the *n/i* and *i/p* interfaces. The *p* layer is normally nc-Si:H for good solar cell performance [30].

The a-SiGe:H cell structure is more complicated than a-Si:H solar cells. First, a-SiGe:H has a lower bandgap than a-Si:H, which causes bandgap discontinuities at the *n/i* and *i/p* interfaces. A buffer layer at the interface is desirable to smoothen the discontinuity. Second, the material quality of a-SiGe:H is poorer than that of a-Si:H because of compositional disorder and the lower Ge-H chemical bonding energy than for Si-H bonds. The defect density increases with the increase of Ge content in the material. Generally speaking, a-SiGe:H solar cells have a poorer FF than a-Si:H for the same intrinsic layer thickness. We have carried out extensive experiments to improve the a-SiGe:H material quality. In parallel, we have tried to minimize the influence of high defect density of a-SiGe:H on the solar cell performance. One such successful approach is the bandgap profiling technique [31], which dynamically changes the Ge/Si ratio during the deposition. Figure 2 shows four bandgap profiles of flat (a), increasing (b), decreasing (c), and double-profiling (d). From the point of view of absorption, the decreasing bandgap profiling (c) should perform better than the increasing bandgap profiling (b), because the short-wavelength light will be absorbed in the *p/i* front region and the long wavelength in the back region. However, from the point of view of carrier transport, the increasing bandgap profiling (b) should be better than the decreasing profiling (c). In this case, most of photo-carriers are generated in the *p/i* region, the holes need to travel only a relatively short distance to reach the *p* layer and the hole collection should be improved. Table 2 lists experimental data of a-SiGe:H solar cells made on stainless steel substrates with the four types of banddgap profiling shown in Fig. 2, where the average Ge/Si ratio was kept the same for all four solar cells. A few observations are made here. First, the decreasing bandgap profiling (c) leads to a high V_{oc} but poor FF, especially the red FF (FF_r). The high V_{oc} results from the wide bandgap near the *p/i* interface, which is the dominant junction of the solar cells. The poor FF is caused by the low hole collection because of the enhanced generation near the *n/i* region. Second, the increasing bandgap profiling (b) increases the FF significantly because of the improved hole collection. However, the V_{oc} is low because of the low bandgap near the *i/p* region. Third, with the double profiling, the FF remains as high as the increasing profiling, and the V_{oc} is also improved. The small region with a decreasing bandgap in the *i/p* region smoothens the bandgap discontinuity and reduces the interface recombination.

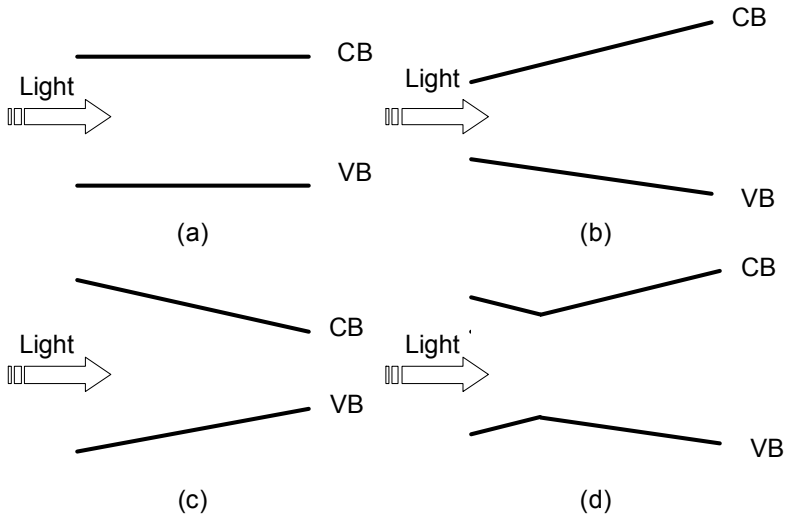

Figure 2. Different types of bandgap profiling for a-SiGe:H solar cells, where (a) is flat bandgap, (b) increased bandgap, (c) decreased bandgap, and (d) double-profiled bandgap.

Downloaded from SPIE Digital Library on 04 Jan 2010 to 159.226.100.225. Terms of Use: http://spiedl.org/terms

Table 2. Light J-V characteristic of a-SiGe:H solar cells with different types of bandgap profiling. The solar cells were measured under an AM1.5 solar simulator and with a 530-nm long pass filter. FF_b and FF_r represent the FF measured with low intensity blue and red lights. P_{max} is the maximum power under the given illuminations.

Bandgap Profiling	Light	J_{sc} (mA/cm^2)	V_{oc} (V)	FF	FF_b	FF_r	P_{max} (mW/cm^2)
(a)	>530	10.25	0.744	0.611			4.66
	AM1.5	15.11	0.760	0.527	0.655	0.592	6.05
(b)	>530	10.49	0.712	0.634			4.74
	AM1.5	15.61	0.729	0.638	0.675	0.642	7.26
(c)	>530	10.02	0.764	0.530			4.06
	AM1.5	15.01	0.785	0.656	0.694	0.501	6.70
(d)	>530	10.49	0.730	0.640			4.90
	AM1.5	15.94	0.748	0.647	0.687	0.640	7.71

2.3. High efficiency a-Si:H/a-SiGe:H/a-SiGe:H triple-junction solar cells

With optimized a-Si:H and a-SiGe:H solar cells, we have studied multi-junction solar cells on the Ag/ZnO back reflector. Combining the component cells into multi-junction structures, two important factors must be taken into consideration. First, since the component cells are connected in series, the voltage is the sum of the voltages from the component cells and the current is limited by the lowest current of a component cell. Therefore, the current mismatching is a key for determining the efficiency of multi-junction solar cells. Without considering the difference of FF and V_{oc} of the component cells, a perfect matched current should give the highest efficiency. However, the difference in FF and V_{oc} also plays an essential role in the current mismatching for high efficiency. Second, in a multi-junction solar cell, the adjacent component cells are connected by a reversed *p/n* junction, where the current flows via carriers tunneling from one type of material to another, and an Ohmic contact is required. Therefore, the internal *p/n* junction is also called the tunnel junction. Experimental results have shown that nanocrystalline doped layers are important to form good tunnel junctions. Our high quality *p*-type nc-Si:H layer has demonstrated to be a good doped layer for the tunnel junction.

Table 3 lists the solar cell performance achieved using various solar cell structures [15], where the active area of the solar cells is 0.25 cm^2, defined by the ITO top contact. The highest initial and stable cell efficiencies achieved are 14.6% and 13.0%, respectively [13] using an a-Si:H/a-SiGe:H/a-SiGe:H triple-junction structure. Figure 3 shows the initial J-V characteristics and quantum efficiency (QE) curves of the triple-junction solar cell. Using the same triple-junction structure, we have also demonstrated in a large area batch machine a stable aperture-area efficiency of 10.5% from an encapsulated cell with an aperture area of 820 cm^2.

Table 3. Initial and stable solar cell J-V characteristics of a-Si:H and a-SiGe:H solar cell structures from United Solar.

Cell structure	State	J_{sc} (mA/cm^2)	V_{oc} (V)	FF	η (%)
a-Si:H single-junction	initial	14.65	0.992	0.730	10.6
	stable	14.36	0.965	0.672	9.3
a-Si:H/a-Si:H double-junction	initial	7.90	1.890	0.760	11.4
	stable	7.90	1.830	0.700	10.1
a-Si:H/a-SiGe:H double-junction	initial	11.04	1.762	0.738	14.4
	stable	10.68	1.713	0.676	12.4
a-Si:H/a-SiGe:H/a-SiGe:H triple-junction	initial	8.57	2.357	0.723	14.6
	stable	8.27	2.294	0.684	13.0

Downloaded from SPIE Digital Library on 04 Jan 2010 to 159.226.100.225. Terms of Use: http://spiedl.org/terms

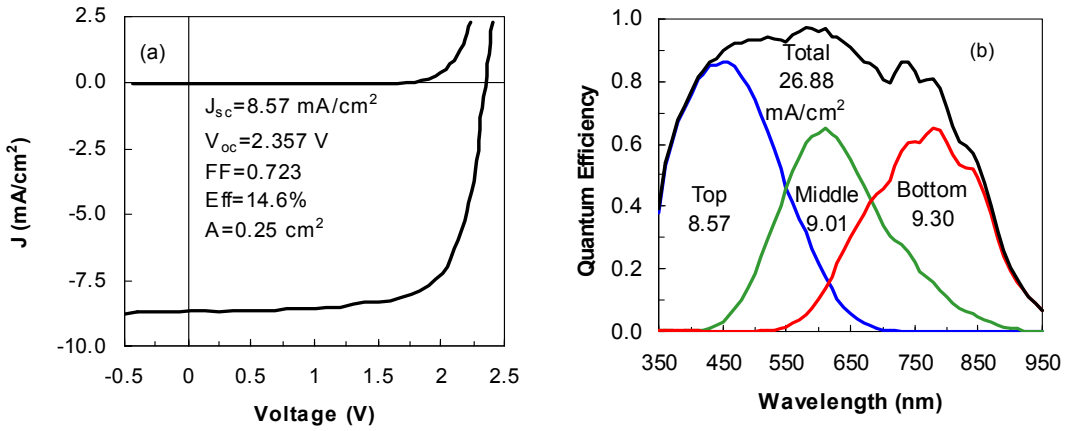

Figure 3. Initial J-V characteristics and QE curves of a high efficiency a-Si:H/a-SiGe:H/a-SiGe:H triple-junction solar cell.

2.4. Roll-to-roll manufacturing process

Based on the a-Si:H/a-SiGe:H/a-SiGe:H triple-junction solar cell structure, United Solar built a roll-to-roll 5MW/year production line in 1997 and the first roll-to-roll 30 MW/year plant in 2003 [7,15,27]. Our current total capacity is 180 MW/year. The deposition system consists of four consecutive roll-to-roll machines: washing, deposition of back reflector, deposition of a-Si:H based triple-junction structure, and deposition of top conductive layer. The a-Si:H deposition machine is shown in Fig. 4, where six rolls of stainless steel substrate go through the deposition system simultaneously at a speed of ~1 cm/s. The length of the 125μm thick stainless steel substrate is ~2.5 kilometers and the width is ~36 cm.

Figure 4. Triple-junction processor located at Auburn Hills, Michigan.

2.5. Assembly process and *Uni-Solar* laminate products

After the deposition, the rolls of solar cells are cut into slabs for assembly processes, including short passivation, bonding of electrodes, cell inter-connection, and lamination. During the assembly process, several inspection steps are carried out to ensure the quality of the product [15]. One major product is the 22-L laminate shown in Fig. 5, which has a power rating of 144 W and carries a 25-year warranty.

Unlike conventional c-Si panels and other thin-film products on glass, *Uni-Solar* laminate products are light weight, flexible, and robust. The characteristics of light weight and flexibility make the product ideal for roof-top applications on commercial and residential buildings. In addition, the installation process is much simpler than other solar products. The rolls of *Uni-Solar* laminates can be easily installed as shown in Fig. 6. Many large installations with *Uni-Solar* laminates have been built around the world.

Downloaded from SPIE Digital Library on 04 Jan 2010 to 159.226.100.225. Terms of Use: http://spiedl.org/terms

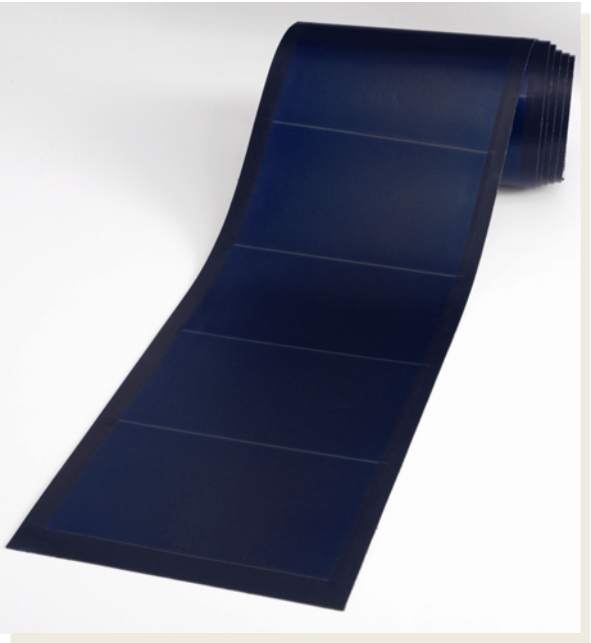

Figure 5. *Uni-Solar*'s flexible solar laminates.

Figure 6. An example of *Uni-Soar* laminates on a rooftop.

3. AMORPHOUS AND NANOCRYSTALLINE SILICON BASED MULTI-JUNCTION SOLAR CELLS

The low material cost and large-scale manufacturability of a-Si:H based solar modules have attracted many industries to this technology. Improvement of conversion efficiency is essential to lowering cost further. Most of a-Si:H solar panels on the market show stable aperture area efficiencies in the range of 5% to 8.5%. Our products have a stable aperture area efficacy ~8.5%, which is the highest among a-Si:H based products. While efforts are under way to improve the efficiency further by improving light trapping, and also by incorporation of superior a-SiGe alloys, nc-Si:H also offers exciting opportunities.

3.1. Nanocrystalline silicon deposition and issues in material optimization

Compared to the a-Si:H and a-SiGe:H materials, nc-Si:H materials have two major advantages in solar cell applications. First, nc-Si:H material is a mixture of nanometer sized grains and amorphous tissues [12]. The carrier transport is mainly through the crystalline paths, where the carrier mobility is much higher. This allows the solar cell to be thick enough for high photocurrent. In addition, the amorphous phase in nc-Si:H absorbs the short wavelength light more efficiently than c-Si:H, while the nanocrystallites absorb the long wavelength lights. Second, nc-Si:H solar cells are more stable against light soaking than a-Si:H and a-SiGe:H solar cells, which can lead to high efficiency solar modules. United Solar has been working on nc-Si:H materials and solar cells since 2001. Over the years, we have encountered but successfully resolved several issues, as described below.

The first issue was an ambient degradation observed in nc-Si:H solar cells without intentional light soaking, which was caused by high porosity in the material [24]. The porous structure in unoptimized nc-Si:H allowed impurities to diffuse into the material and degrade the cell performance. In some cases, the ambient degradation was so severe that it was readily observed even in an a-Si:H/nc-Si:H double-junction cell, where even the top a-Si:H cell could not block the impurity diffusion. The porous structure of the nc-Si:H caused micro-cracks of the a-Si:H top cell and degraded the a-Si:H/nc-Si:H double-junction cell. We investigated the deposition parameters and successfully reduced the porosity in the nc-Si:H and improved the cell performance.

Downloaded from SPIE Digital Library on 04 Jan 2010 to 159.226.100.225. Terms of Use: http://spiedl.org/terms

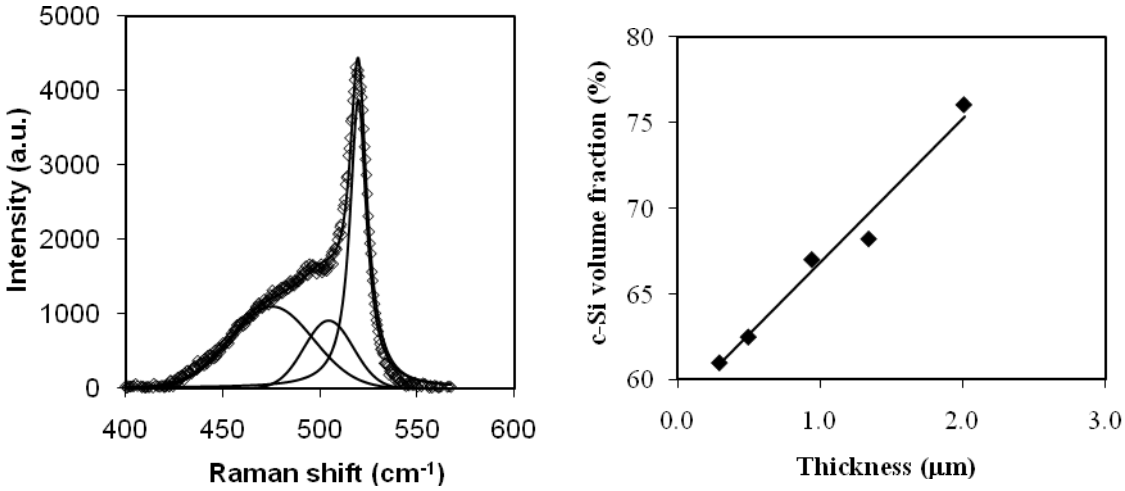

Figure 7. (left) Raman spectrum of a nc-Si:H solar cell with three components of the decomposition and (right) the crystalline volume fraction versus cell thickness.

The second issue concerns nanocrystalline evolution. It has been reported that nc-Si:H materials made under the conditions close to the nanocrystalline to amorphous transition have a compact structure and the corresponding solar cells showed high efficiencies [32]. This phenomenon implies that the nc-Si:H with a high crystalline volume fraction normally contains a high defect density, presumably resulting from poor grain boundary passivation and post-oxidation through the porous structure. The crystalline volume fraction increases with the nc-Si:H thickness [33]. An example is given in Fig. 7, where the plot on the left is a Raman spectrum from a nc-Si:H solar cell and the one on the right is the crystalline volume fraction estimated from decomposition of the Raman spectra for cells with different intrinsic layer thicknesses. It clearly shows that the crystalline volume fraction increases with the film thickness. Such increase of crystalline volume fraction causes the poor nc-Si:H solar cell performance. To resolve the nanocrystalline evolution issue in nc-Si:H solar cells, we have developed a hydrogen dilution profiling technique to control the crystallinity evolution along the growth direction [33]. Because the amorphous to nanocrystalline transition and the crystallinity depend on the hydrogen dilution during the deposition, one can enhance the nanocrystalline formation using very high hydrogen dilution during the initial deposition and suppress the increase of crystallinity by dynamically reducing the hydrogen dilution during the deposition. Experimental results showed that a proper hydrogen dilution profile improves all the three J-V characteristic parameters of J_{sc}, V_{oc}, and FF. Currently, our best nc-Si:H solar cells have slightly inversed crystallinity distribution as shown in Fig. 8, where the crystallinity is higher in the bottom region (near the *n/i* region) than in the top region (near the *i/p* region) [34].

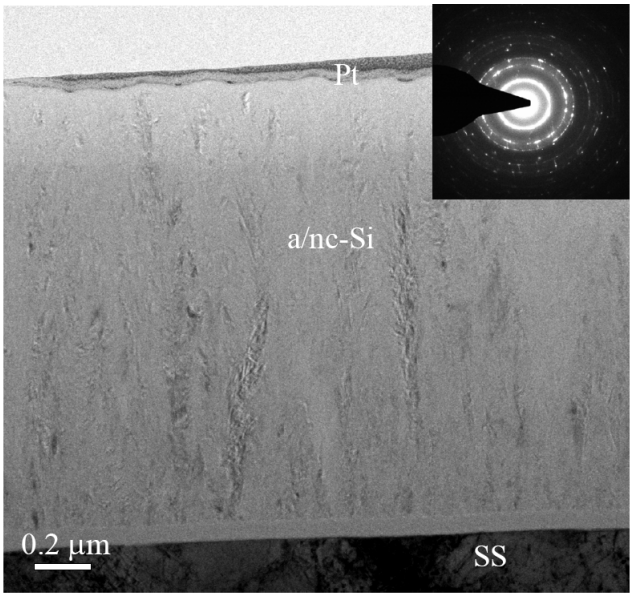

Figure 8. An X-TEM image of nc-Si:H solar cell on SS substrate. A hydrogen profiling is used to create a slightly inversed nanocrystalline distribution.

The most challenging issue is the high rate deposition. We have investigated three methods for depositing nc-Si:H solar cells at high rates, including RF, VHF, and microwave glow discharge [19]. Using RF glow discharge, we can reach the deposition rate of 0.5 nm/s and reasonable solar cell performance. The nc-

Downloaded from SPIE Digital Library on 04 Jan 2010 to 159.226.100.225. Terms of Use: http://spiedl.org/terms

Si:H solar cell performance decreased with the deposition rate even when the high pressure, high power approach was used. Microwave glow discharge can deposit nc-Si:H at very high rates. We have demonstrated 3-4 nm/s deposition rates for nc-Si:H solar cells, but the nc-Si:H performance was not as good as desired. Recently, microwave glow discharge has been investigated again by several other groups. The nc-Si:H deposition rate has been increased even further with optimized system designs. However, good nc-Si:H solar cells have yet to be demonstrated. At United Solar, we are currently using VHF glow discharge to deposit nc-Si:H solar cells at rates of ~1.0-1.5 nm/s.

3.2. Single-junction nanocrystalline silicon solar cell structure

Compared to a-Si:H, the structure of nc-Si:H solar cells is more complex. Figure 9 shows the nc-Si:H solar cell structure used in our laboratory. On top of the *n* layer, an a-Si:H buffer layer is used to reduce P incorporation into the nc-Si:H intrinsic layer. Then, a seed layer made with very high hydrogen dilution is deposited to promote the nucleation of the nc-Si:H intrinsic layer and remove the amorphous incubation layer. As shown in Fig. 8, no a-Si:H incubation layer is observed in the actual solar cell prepared in our laboratory. As discussed in the previous section, the nc-Si:H intrinsic layer is normally made with an appropriate hydrogen dilution to control the nanocrystalline evolution and reach a desired crystallinity distribution along the thickness. An a-Si:H buffer layer was inserted between the nc-Si:H intrinsic layer and the *p* layer to reduce the shunt current and improve the open-circuit voltage (V_{oc}). Although the optimization of each layer is important for the nc-Si:H solar performance, the *i/p* buffer layer is critical for the solar cell performance. As reported previously [34, 35], a thin a-Si:H *i/p* buffer layer cannot reduce the shunt current, which causes poor V_{oc} and FF. If the a-Si:H *i/p* buffer layer is too thick, the carriers cannot be injected into the intrinsic layer efficiently. The result is that the dark J-V cannot turn on properly, and the dark and light J-V curves cross over. As a result, poor FF is observed. The thickness of the a-Si:H *i/p* buffer layer can be experimentally optimized.

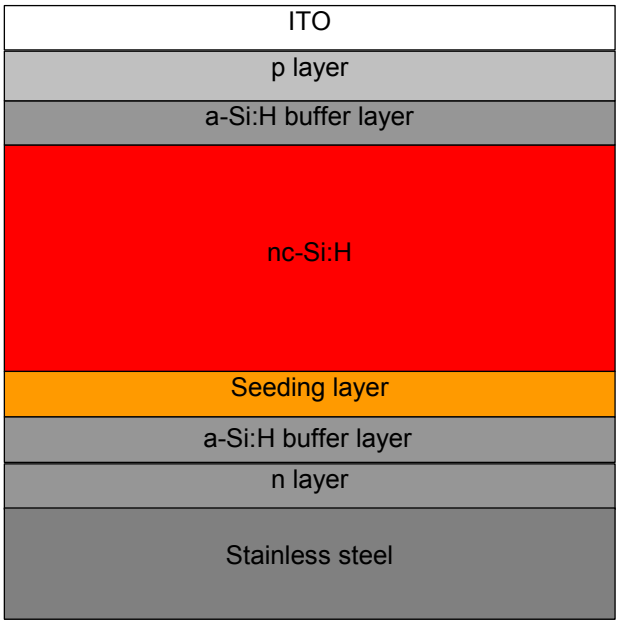

Figure 9. Schematic of nc-Si:H single-junction solar cell structure.

In high efficiency nc-Si:H solar cells, light trapping plays a significant role in enhancing the photocurrent. Many light trapping approaches for nc-Si:H solar cells have been proposed and studied, such as periodic grating structures, photonic back reflectors, and metal nano-particles. We found that all these new approaches have not demonstrated J_{sc} higher than achieved by randomized Ag/ZnO back reflectors. By optimizing the Ag and ZnO textures, we have demonstrated a photocurrent enhancement of 60-75% in nc-Si:H solar cells. The highest J_{sc} is 29.2 mA/cm^2, achieved in a nc-Si:H single-junction solar cell with a 2.5 μm thick nc-Si:H intrinsic layer deposited at 1.0-1.5 nm/s. As compared to the maximum optical enhancement of $4n^2$ (n is the refractive index of silicon) calculated by statistic optics, we are approaching the practical limit of light trapping in nc-Si:H solar cells using randomized back reflectors.

Combining the high quality nc-Si:H materials, optimized solar cell design, and improved Ag/ZnO back reflectors, we have achieved an initial active-area solar cell efficiency of 9.5%; the J-V and QE curves are shown in Fig. 10 [36].

3.3. High efficiency a-Si:H, a-SiGe:H, and nc-Si:H multi-junction solar cells

Using the optimized a-Si:H, a-SiGe:H, and nc-Si:H component cells, we have investigated various multi-junction structures such as a-Si:H/nc-Si:H double-junction, a-Si:H/a-SiGe:H/nc-Si:H triple-junction, and a-Si:H/nc-Si:H/nc-Si:H triple-junction. The highest initial active-area efficiency is 15.4% achieved using the a-Si:H/a-SiGe:H/nc-

Downloaded from SPIE Digital Library on 04 Jan 2010 to 159.226.100.225. Terms of Use: http://spiedl.org/terms

Si:H triple-junction. Figure 11 shows the J-V characteristics of the high efficiency triple-junction solar cell. Table 4 lists the initial and stable J-V data of multi-junction solar cell structures achieved in United Solar [34].

3.4. Large-area deposition of amorphous and nanocrystalline based multi-junction solar cells

We initially tested a-Si:H/nc-Si:H double-junction solar cells using a large-area batch machine with RF glow discharge at a deposition rate of ~0.5 nm/s. In initial and stable aperture area efficiency of 10.5% and 9.5% were achieved on 420 cm^2 [37]. Recently, we have developed large area VHF deposition systems [38]. With knowledge learned from the small area nc-Si:H solar cell optimization, we have made a-Si:H/nc-Si:H double-junction solar cells at high deposition rates > 1.0 nm/s. Table 5 lists examples of our current large-area cell performance, where the solar cells were encapsulated using similar process as in our production lines. The initial cell performances of a-Si:H/nc-Si:H double-junction and a-Si:H/nc-Si:H/nc-Si:H triple-junction solar cells are very similar. However, the light induced degradation is significantly different. For the double-junction solar cells, the light-induced degradation is ~15%, while it is less than 5% for the triple-junction solar cells. With the triple-junction structure, we have achieved stable aperture-area (400 cm^2) cell efficiency of 10.0%. Further improvements in the cell efficiency and large area uniformity are in progress.

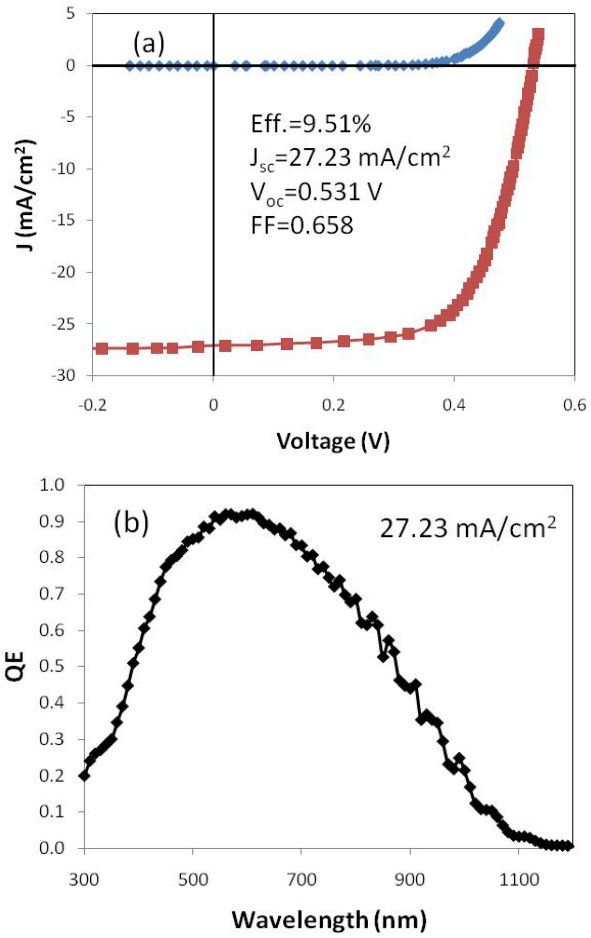

Figure 10. (a) J-V characteristics and (b) quantum efficiency of a nc-Si:H single-junction solar cell on Ag/ZnO back reflector.

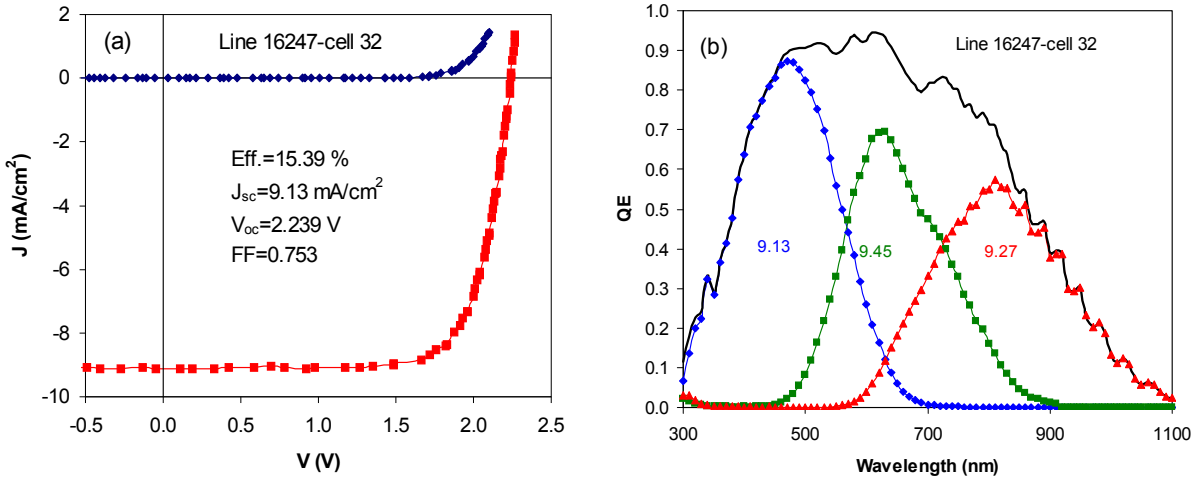

Figure 11. (a) J-V characteristics and (b) quantum efficiency curves of an a-Si:H/a-SiGe:H/nc-Si:H triple-junction cell with an initial active-area efficiency of 15.4%.

Downloaded from SPIE Digital Library on 04 Jan 2010 to 159.226.100.225. Terms of Use: http://spiedl.org/terms

Table 4. Initial and light soaked J-V characteristic of three different multi-junction solar cells with nc-Si:H bottom cells. The data represent the highest efficiencies achieved at United Solar.

Cell structure	State	J_{sc} (mA/cm^2)	V_{oc} (V)	FF	Eff (%)
a-Si:H/nc-Si:H double-junction	Initial	12.61	1.439	0.741	13.5
	Stable	12.22	1.399	0.691	11.8
a-Si:H/a-SiGe:H/nc-Si:H triple-junction	Initial	9.13	2.239	0.753	15.4
	Stable	8.72	2.134	0.716	13.3
a-Si:H/nc-Si:H/nc-Si:H triple-junction	Initial	9.11	1.965	0.790	14.1
	Stable	8.79	1.947	0.771	13.3

Table 5. Initial J-V characteristics of large-area encapsulated nc-Si:H based multi-junction solar cells made using MVHF plasma deposition. The aperture area is 400 cm^2.

Cell structure	Cell #	V_{oc} (V)	J_{sc} (mA/cm^2)	FF	P_{max} (W)	Eff (%)
a-Si:H/nc-Si:H double-junction	14333	1.38	11.5	0.64	4.07	10.2
	14334	1.41	11.5	0.64	4.25	10.6
a-Si:H/nc-Si:H/nc-Si:H triple-junction	14710	1.88	7.8	0.71	4.19	10.5
	14716	1.88	7.8	0.71	4.17	10.4

4. FUTURE PERSPECTIVE OF THIN FILM SILICON SOLAR CELLS

United Solar has been manufacturing multi-junction solar modules since 1986. From a pilot plant production of ~600 kW in 1986, it has emerged as the largest manufacturer of solar laminates having an annual production capacity of 180 MW. The spectrum splitting a-Si:H/a-SiGe:H/a-SiGe:H triple-junction cell structure is being used in all the current manufacturing plants. For the nc-Si:H based technology, technical issues such as high conversion efficiency, high deposition rate, and large-area deposition uniformity, as well as the manufacturing cost need to be addressed prior to consideration for manufacturing. The first issue is to achieve higher efficiency than the current product. The highest small area cell efficiency achieved with a-Si:H/nc-Si:H/nc-Si:H triple-junction solar cells is only slightly higher than the champion cell achieved in a-Si:H/a-SiGe:H/a-SiGe:H triple-junction solar cells. For large-area modules, we have not demonstrated that the efficiency of multi-junction cells with nc-Si:H is much higher than the a-Si:H and a-SiGe:H triple-junction structure. In order to make a sound business decision, we believe that at least a 10% improvement in the cell performance is needed. We have yet to reach the efficiency requirement.

The second issue is to increase the nc-Si:H deposition rate. For the same manufacturing machine length, the deposition rate of nc-Si:H needs to be at least 2.0 nm/s if an a-Si:H/nc-Si:H/nc-Si:H triple-junction structure is to be used. Currently, the deposition rate of nc-Si:H intrinsic layer is ~1.0-1.5 nm/s. Significant effort is needed to increase the deposition rate.

The third issue is the large-area uniformity. VHF has been shown as a possible method for the intrinsic nc-Si:H deposition. However, the large-area uniformity is a great challenge for the cathode design, especially if one desires to use high pressure/high power depleting regime for increasing the deposition rate.

The above three areas are identified as the major future research topics for the development of a-Si:H and nc-Si:H based photovoltaic technology. We need to demonstrate that by integrating a-Si:H and nc-Si:H in a multi-junction structure, stable module efficiencies of larger than10% and 11% can be achieved with Al/ZnO and Ag/ZnO back

Downloaded from SPIE Digital Library on 04 Jan 2010 to 159.226.100.225. Terms of Use: http://spiedl.org/terms

reflectors, respectively, when the nc-Si:H layer is deposited at > 1.5 nm/s. We also need to design and test various VHF cathodes to achieve uniform large-area nc-Si:H deposition, and evaluate the a-Si:H and nc-Si:H deposition process in a roll-to-roll machine. We are following a stage gate process to introduce nc-Si:H in manufacturing.

5. SUMMARY

We have reviewed United Solar's a-Si:H/a-SiGe:H/a-SiGe:H triple-junction photovoltaic technology, which has been developed over the past three decades. The material properties have been optimized as a function of various deposition parameters. The solar cell design is also optimized by improving the photo-carrier collection. Two major technical approaches are essential in achieving high efficiency solar cells: hydrogen dilution to improve the material quality and bandgap profiling to improve the solar cell design. With the advanced triple-junction solar cell structure, we have witnessed several generations of roll-to-roll manufacturing lines for flexible and light weight products. Our current manufacturing capability is 180 MW. Future expansion of the manufacturing capacity is being pursued.

In order to develop even higher module efficiencies, we have carried out systematic studies on nc-Si:H solar cells. We made a new world record cell efficiency with an a-Si:H/a-SiGe:H/nc-Si:H triple-junction structure. The deposition rate for nc-Si:H has been increased to ~1.5 nm/s. The stable aperture-area module efficiency of 10.0% has also been achieved using a high deposition rate. To implement the nc-Si:H based solar cells into large volume manufacturing, we need to make significant improvement in three areas: efficiency, deposition rate, and large-area deposition uniformity.

ACKNOWLEDGMENTS

We thank the entire Research and Development Department at United Solar for their contribution and great teamwork, especially to Baojie Yan and Guozhen Yue for their help in the preparation of the manuscript. This work was supported by US DOE under SAI Program contract No. DE-FC36-07 GO 17053.

REFERENCES

[1] Deb, S. K., "Recent Advances and Future Opportunities for thin-film solar cells" in [Thin-Film Solar Cells-Next Generation Photovoltaics and Its Applications], edited by Hamakawa, Springer, Berlin, 15-42 (2004).

[2] Meier, J., Kroll, U., Benagli, S., Roschek, T., Huegli, A., Spitznagel, J., Kluth, O., Borello, D., Mohr, M., Zimin, D., Monteduro, G., Springer, J., Ellert, C., Androutsopoulos, G., Buechel, G., Zindel, A., Baumgartner, F., and Koch-Ospelt, D., "Recent progress in up-scaling of amorphous and micromorph thin film silicon solar cells to 1.4 m^2 modules", Mater. Res. Soc. Symp. Proc. 989, 545-556 (2007).

[3] Delahoy, A.E., Guo, S., Stavrides, A., Patel, A., Cambridge, J., Xu, Y., Varvar, A., Berens, T., Twesme, E., Iafelice, V., Johnson, B., Steiger, R., Le, L., Jansen, K., and Eichelbroenner, M., "Status of amorphous silicon at epv solar: module manufacturing, device performance, and R&D", 23rd European Photovoltaic Solar Energy Conf., 2069-2074 (2008).

[4] Takano, A., Tabuchi, K., Uno, M., Tanda, M., Wada, T., Shimosawa, M., Sakakibara, Y., Kiyofuji, S., Nishihara, H., Enomoto, H., and Kamoshita, T., "Production Technologies of Film Solar Cell", Mater. Res. Soc. Symp. Proc. 910, 687-696 (2006).

[5] Fukuda, S., Yamamoto, K., Nakajima, A., Yoshimi, M., Sawada, T., Suezaki, T., Ichikawa, M., Koi, Y., Goto, M., Meguro, T., Matsuda, T., Sasaki, T., and Tawada, Y., "High efficiency thin film silicon hybrid cell and module with newly developed interlayer", Proc. of 21st European Photovoltaic Solar Energy Conference, 1535-1538 (2006).

[6] Takatsuka, H., Yamauchi, Y., Takeuchi. Y., Fukagawa, M., Kawamura, K., Goya, S., and Takano, A., "The world's largest high efficiency thin film silicon solar cell module", Conf. Record of the 2006 IEEE 4th World Conf. on Photovoltaic Energy Conversion, 2026-2033 (2006).

[7] Izu, M., and Ellison, T., "Roll-to-roll manufacturing of amorphous silicon alloy solar cells with in situ cell performance diagnostics", Sol. Energy Mater. & Sol. Cells 78(1-4), 613–626 (2003).

[8] Saito, K., Sano, M., Okabe, S., Sugiyama, S., and Ogawa, K., "Microcrystalline silicon solar cells fabricated by VHF plasma CVD method", Sol. Energy Mater. & Sol. Cells 86(4), 565–575 (2005).

Downloaded from SPIE Digital Library on 04 Jan 2010 to 159.226.100.225. Terms of Use: http://spiedl.org/terms

[9] Staebler, D. L. and Wronski, C. R., "Reversible conductivity changes in discharge-produced amorphous Si", Appl. Phys. Lett. 31(4), 292-294 (1977).
[10] Yang, J., Banerjee, A., and Guha, S., "Triple-junction amorphous silicon alloy solar cell with 14.6% initial and 13% stable conversion efficiencies", Appl. Phys. Lett. 70(22), 2975-2978 (1997).
[11] Guha, S. and Yang, J., Banerjee, A., and Sugiyama, S., "Material Issues in the Commercialization of amorphous silicon ally thin-film photovoltaic technology", Mater. Res. Soc. Symp. Proc. 507, 99-105 (1998).
[12] Yang, J., Banerjee, A., and Guha, S., "Amorphous silicon based photovoltaics-from earth to the *final frontier*", Sol. Energy Mater. & Sol. Cells 78(1-4), 597–612 (2003).
[13] Meier, J., Flückiger, R., Keppner, H., and Shah, A., "Complete microcrystalline *p-i-n* solar cell-crystalline or amorphous cell behavior?", Appl. Phys. Lett. 65(7), 860-862 (1994).
[14] Meier, J., Torres, P., Platz, R., Dubail, S., Kroll, U., Selvan, J.A.A., Pellaton-Vaucher, N., Hof, C., Fischer, D., Keppner, H., Shah, A., Ufert, K.-D., Giannoules, P., and Kohler, J., "On the way towards high efficiency thin film silicon solar cells by "micromorph" concept", Mater. Res. Soc. Symp. Proc. 420, 3-15 (1996).
[15] Shah, A.V., Meier, J., Vallat-Sauvain, E., Wyrsch, N., Kroll, U., Droz, C., and Graf, U.," Material and solar cell research in microcrystalline silicon", Sol. Energy Mater. & Sol. Cells 78(1-4), 469–491 (2003).
[16] Yan, B., Yue, G., Yang, J., Banerjee, A., and Guha, S., "Hydrogenated microcrystalline silicon single-junction and multi-junction solar cells", Mater. Res. Soc. Symp. Proc. 762, 309-320 (2003).
[17] Yan, B., Yue, G., Owens, J. M., Yang, J., Banerjee, A., and Guha, S., "Over 15% Efficient Hydrogenated Amorphous Silicon Based Triple-Junction Solar Cells Incorporating Nanocrystalline Silicon", Conf. Record of the 2006 IEEE 4th World Conf. on Photovoltaic Energy Conversion,1477-1480 (2006).
[18] Yan, B., Yue, G., and Guha, S., "Status of nc-Si:H solar cells at United Solar and roadmap for manufacturing a-Si:H and nc-Si:H based solar panels", Mater. Res. Soc. Symp. Proc. 989, 335-346 (2007).
[19] Yan, B., Yue, G., Yang, J., Lord, K., Banerjee, A., and Guha, S., "Microcrystalline silicon solar cells made using RF, MVHF, and microwave at various deposition rates", Proc. of 3rd World Conference on Photovoltaic Energy Conversion, 2773-2777 (2003).
[20] Jia, H., Shirai, H., and Kondo, M., "Fast deposition of highly crystallized microcrystalline Si films utilizing a high-density microwave plasma source for si thin film solar cells", Mater. Res. Soc. Symp. Proc. 910, 309-315 (2006).
[21] Löffler, L., Devilee, C., Geusebroek, M., Soppe, W. J., and Muffler H.-J., "Deposition of μc-Si:H by microwave PECVD– influence of process conditions on layer properties", Proc. of 21st European Photovoltaic Solar Energy Conference, 1597-1600 (2006).
[22] van de Sanden, M.C.M., Severens, R.J., Kessels, W.M.M., Meulenbroeks, R.F.G., and Schram, D.C., "Plasma chemistry aspects of a-Si:H deposition using an expanding thermal plasma", J. Appl. Phys. 84(5), 2426-2435 (1998).
[23] Mahan, A. H., "Hot wire chemical vapor deposition of Si containing materials for solar cells", Sol. Energy Mater. & Sol. Cells 78(1-4), 299-3 (2003).
[24] Yan, B., Lord, K., Yang, J., Guha, S., Smeets, J., and Jacquet, J.-M., "Hydrogenated microcrystalline silicon solar cells made with modified very-high-frequency glow discharge", Mater. Res. Soc. Symp. Proc. 715, 629-635 (2002).
[25] Guha, S., Narasimhan, K. L., and Pietruszko, S. M., "On light-induced effect in amorphous hydrogenated silicon", J. Appl. Phys. 52(2), 859- 860(1981).
[26] Lord, K., Yan, B., Yang, J., and Guha, S., "Light-induced increase in the open-circuit voltage of thin-film heterogeneous silicon solar cells", Appl. Phys. Lett. 79(23), 3800 (2001).
[27] Guha, S. Yang, J., Banerjee, A., Yan, B., and Lord, K., "High quality amorphous silicon materials and cells grown with hydrogen dilution", Sol. Energy Mater. & Sol. Cells 78(1-4), 329 (2003).
[28] Tsu, D.V., Chao, B. S., Ovshinsky, S. R., Yang, J., and Guha, S., "Effect of hydrogen dilution on the structure of amorphous silicon alloys", Appl. Phys. Lett. 71(10), 1317-1319 (1997).
[29] Owens, J. M., Han, D., Yan, B., Yang, J., Lord, K., and Guha, S., "Micro-Raman studies of mixed-phase hydrogenated silicon solar cells", Mater. Res. Soc. Symp. Proc. 762, 339-345 (2003).
[30] Guha, S., Yang, J., Nath, P., and Hack, M., "Enhancement of open circuit voltage in high efficiency amorphous silicon alloy solar cells", Appl. Phys. Lett. 49(4), 218-221 (1986).
[31] Guha, S., Yang, J., Pawlikiewicz, A., Glatfelter, T., Ross, R., and Ovshinsky, S. R., "Band gap profiling for improving the efficiency of amorphous silicon alloy solar cells", Appl. Phys. Lett. 54(23), 2330-2332 (1989).

Downloaded from SPIE Digital Library on 04 Jan 2010 to 159.226.100.225. Terms of Use: http://spiedl.org/terms

[32] Roschek, T., Repmann, T., Müller, J., Rech, B., and Wagner, H., "High rate deposition of microcrystalline silicon solar cells using 13.56 MHz PECVD ", Proc. of 28th IEEE Photovoltaic Specialists Conference, Anchorage, 150-153(2000).

[33] Yan, B., Yue, G., Yang, J., Guha, S., Williamson D. L., Han, D., and Jiang C.-S., "Hydrogen dilution profiling for hydrogenated microcrystalline silicon solar cells", Appl. Phys. Lett. 85(11), 1955-1957 (2004).

[34] Yan, B., Yue, G., Yan, Y., Jiang, C.-S., Teplin, C. W., Yang, J., and Guha, S., "Correlation of hydrogen dilution profiling to material structure and device performance of hydrogenated nanocrystalline silicon solar cells", Mater. Res. Soc. Symp. Proc. 1066, 61-66 (2008).

[35] Yue, G., Yan, B., Teplin, C. W., Yang, J., and Guha, S., "Optimization and characterization of *i/p* buffer layer in hydrogenated nanocrystalline silicon solar cells", J. Non-Crystal Solids, 354(19-25), 24402443 (2008).

[36] Yue, G., Yan, B., Sivec, L., Owens, J. M., Hu, S., Xu, X., Yang, J., and Guha, S., "Improvement of a-Si:H and nc-Si:H multi-junction solar cells by optimization of textured back reflectors", Proc. 34th IEEE Photovotaics Energy Conversion Specialists Conferences, (2009).

[37] Yan, B., Yue, G., Banerjee, A., Yang, J., and Guha, S., "Large-area hydrogenated amorphous and microcrystalline silicon double-junction solar cells", Mater. Res. Soc. Symp. Proc. 808, 581-586 (2004).

[38] Xu, X., Su, T., Beglau, D., Ehlert, S., Pietka, G., Bobela, D., Li, Y., Lord, K., Yue, G., Zhang, J., Yan, B., Worrel, C., Beernink, K., DeMaggio, D., Banerjee, A., Yang, J., and Guha, S., "High efficiency large area multi-junction solar cells incorporating a-SiGe:H and nc-Si:H using MVHF technology", Proc. 34th IEEE Photovotaics Energy Conversion Specialists Conferences, (2009).

Downloaded from SPIE Digital Library on 04 Jan 2010 to 159.226.100.225. Terms of Use: http://spiedl.org/terms